Criteria for Ultrastable Operation of the Trapped Ion Frequency Standard

R. L. Tjoelker, J. D. Prestage, and L. Maleki
Communications Systems Research Section

The leading systematic perturbations to the JPL mercury trapped ion frequency standard under present operating conditions are characterized. Sensitivity of the standard to environmental variations is measured, and the required regulation of key components to obtain a stability of 10^{-16} is identified.

I. Introduction

The 40.5-GHz atomic ground-state hyperfine "clock" transition of $^{199}Hg^{+}$ [1] has been measured in the JPL trapped ion frequency standard to have a corresponding line $Q \equiv \nu/\Delta\nu$ greater than 10^{12}, the highest ever measured in a microwave transition. A good signal to noise ratio (SNR) is achieved with as many as 3×10^{7} ions in a linear ion trap (LIT)[5]. This high Q, together with improved SNR, has resulted in a demonstrated performance of $1 \times 10^{-13}/\sqrt{\tau}$ [2,3] where τ represents the averaging time interval.

The achievement of long-term stability depends upon the sensitivity to, and degree of isolation from, external influences. Because of their large mass and large hyperfine splitting, mercury ions provide a standard that, in general, is much less sensitive to environmental variations than hydrogen and cesium. Though sensitivities are greatly reduced, several offsets of the Hg^{+} clock-transition frequency still exist under practical operating conditions. The obtainable long-term stability depends directly on the stabilization of these offsets. Under the present operating conditions, the fractional frequency stability of the trapped ion standard has been measured to be better than 2×10^{-15} with 24,000-sec averaging times [2,3].

In this article, the leading perturbations and limitations to the present performance of the JPL mercury trapped ion frequency standard are quantified. Environmental sensitivity of the standard is measured, and the operating parameters required to reach a long-term stability of 10^{-16} are identified.

II. Operation of the Ion Trap Standard

In the present operational configuration (Figs. 1 and 2), $^{199}Hg^{+}$ ions are created inside the trap by an electron pulse along the trap axis, which ionizes a neutral background vapor of ^{199}Hg obtained by heating isotopically purified ($\approx$ 96-percent) HgO powder. Collisions with a helium buffer gas ($\approx 10^{-5}$ mbar) cool the ions to thermal equilibrium with the vacuum enclosure, currently kept at room temperature. Resonance ultraviolet radiation (UV) (194.2 nm) from a ^{202}Hg discharge lamp optically pumps the ions into the $F = 0$ hyperfine level of the ground state. To minimize scattered light, the state-selection light is collected in a pyrex horn. Microwave radiation (40.5 GHz)

to transfer the population to the $F = 1$ ground state enters the trap region through the pyrex horn and in a direction opposite to the UV state selection/interrogation light. This allows collection of atomic fluorescence in both directions perpendicular to the incident pumping light. Currently, fluorescence is collected in only one of these two directions. Inclusion of a second light-collection system should improve the SNR by $\sqrt{2}$.

The loading, state preparation, and interrogation cycle has been previously described [6]. After the $^{199}Hg^{+}$ ions are pumped into the $^2S_{1/2}(F = 0, m = 0)$ state, the technique of successive oscillatory fields [4] is used to probe the approximately 40.5-GHz hyperfine clock transition to the $^2S_{1/2}(F = 1, m = 0)$ state, Fig. 6(a). It is necessary to switch the UV state-selection/interrogation light level to near zero during the microwave interrogation period to prevent light shifts and broadening of the clock transition. After application of the second microwave pulse, the UV light is again turned back on to determine if the microwaves were on resonance and if they successfully transferred the population to the $F = 1$ state. A background light level between 10^5 and 5×10^5 counts per 1.0-sec collection period is subtracted to observe the resonance.

III. System Sensitivity and Systematics

A. Second-Order Doppler Shift

The largest frequency perturbation in standards based on ions confined in rf ion traps typically results from the motion of the ions (micromotion) due to the oscillating trapping fields via the second-order Doppler effect (relativistic time dilation). In order to increase the number of stored ions with little corresponding increase in second-order Doppler shift, a hybrid rf/dc linear ion trap is used [5]. This trap confines ions along a nodal line of the rf field. The trapping force transverse to the nodal line is generated by the ponderomotive force as in conventional hyperbolic Paul traps, while the axial trapping force is provided by dc electric fields.

Since the distance from the nodal line determines the magnitude of the rf trapping field, the second-order Doppler shift is reduced from that of a hyperbolic trap for the same number of ions by a factor of $(5/3)R_{\rm sph}/L$, where $R_{\rm sph}$ is the radius of a hyperbolic trap and L is the length of the linear ion trap. Ions in a long linear trap (where end effects are negligible) show a second-order Doppler shift of

$$\left(\frac{\Delta f}{f}\right)_{\rm lin} = -\left(\frac{q^2}{8\pi\epsilon_o mc^2}\right)\frac{N}{L} \qquad (1)$$

where N/L is the linear number density of ions in the trap [5]. For mercury, this fractional frequency shift is

$$\left(\frac{\Delta f}{f}\right)_{\rm Hg} = -\left(3.8 \times 10^{-21}\ \text{meters}\right)\frac{N}{L} \qquad (2)$$

Within the linear trap, the absolute second-order Doppler shift due to the trapping fields is greatly reduced, while allowing for an increased ion number and SNR.

Confinement lifetimes ranging from 2000–14,500 sec have been measured, depending upon the trap's well depth and background pressure. Even though the second-order Doppler shift and the sensitivity to ion-number fluctuations is reduced by using the linear ion trap, for ultrastable operation it still is necessary to keep the number of ions (N) in the trap fixed. The number is kept nearly constant (better than 0.1 percent) through repeated loading of the trap, though currently there is no active number stabilization. Once each interrogation cycle [6] (ranging from $\approx$ 5–30 sec), a filament is pulsed, which emits electrons to ionize the neutral mercury in the trapping region. The equilibrium ion number is attained when the loading rate and loss rate are equal. The stability of the ion number over very long times depends on the stability of the background pressure of neutral mercury, filament emission, electron energy, electron pulse duration and duty cycle, and trap potentials (rf and dc). For the data presented in [2,3], these parameters have been regulated to a level summarized in Table 1. When the ionizing electrons are turned off, the number-dependent second-order Doppler shift from ion motion is directly observed by measuring the clock frequency as the ion number N decays (Fig. 3). By using Eq. (1) the measured frequency offset of 1.5×10^{-12} corresponds to about 3×10^7 ions, with the endcap potential of $V_{\rm EC} = 10$ V.

If the background mercury pressure and electron pulse duration are sufficiently large, some passive stabilization is apparently achieved by filling the trap to a saturation level for a given voltage on the end electrodes. These electrodes are thin needles with a diameter of 2 mm [5]. Depending on the geometric details, the endcap electrodes can provide a limiting radius beyond which ions are no longer confined [7]. Under present operating conditions, the number stability is better than 0.1 percent, based on the measured stability of 2×10^{-15} over the 24,000-sec averaging times [2,3].

In Fig. 4(a), the frequency shift as a function of the potential $V_{\rm EC}$ on the endcaps is shown. This shift corresponds to a change in the average ion cloud radius. Figure 4(b) shows the measured peak amplitude (observed flu-

orescence) of the clock resonance versus the same variation in endcap voltage. This suggests that the frequency offset in Fig. 4(a) is due in part to variations in Hg^+ number. Further analysis of the potentials may provide a higher degree of number control in a passive way—a useful feature for a practical frequency standard.

B. Background Pressure Shifts

A buffer gas of neutral helium is used to cool and keep the Hg^+ ions in near-thermal equilibrium with the room-temperature vacuum enclosure. Slowing and cooling the ions allows them to become bound in the trap and reduces the radial extent of a given ion cloud, thus reducing the second-order Doppler shift. However, collisions between the mercury and helium buffer gas perturb the mercury hyperfine transition. The measured fractional frequency offset corresponding to helium pressure for a fixed set of loading conditions is shown in Fig. 5.

This dependence was first discussed by Cutler et al. [8]. At low pressures the quantity of helium is not sufficient to cool the trapped ions into thermal equilibrium with the vacuum enclosure. Instead, the mercury temperature rises with reduced helium pressure, which produces an increased thermal second-order Doppler shift of $3.2 \times 10^{-12}/10^{-5}$ mbar. For helium pressures higher than 6×10^{-6} mbar, the sensitivity is reduced to $1.1 \times 10^{-13}/10^{-5}$ mbar. In this region, the mercury ions are in thermal equilibrium and the predominant frequency dependence is a hyperfine shift due to collisions [9]. Currently, the helium pressure is measured with an ionization gauge, and the measured level is used to servo the heater of a quartz helium leak to hold the pressure constant. To reduce sensitivity to pressure fluctuations, yet operate with as little helium as possible, the operating pressure is typically 8×10^{-6} mbar.

In the present vacuum configuration (Fig. 1), the trap region is differentially pumped to a 40 l/sec turbo pump and the HgO source cannot be isolated from the trap vacuum. The partial helium pressure of 8×10^{-6} mbar constitutes the largest component of the background gas. The partial pressure of neutral ^{199}Hg is about 10^{-10} mbar. The helium is responsible for a fractional frequency offset of about 10^{-13}, and the presence of mercury (and presumably oxygen) most likely also perturbs the absolute frequency, though to a lesser extent, by several orders of magnitude.

Recently other gas contaminants have been reported to contribute significant systematic shifts in microwave atomic frequency standards. At the National Institute of Standards and Technology (NIST), a pressure-related shift of $\approx 10^{-13}$ has been reported in the Be^+ hyperfine clock transition due to a 10^{-10}-mbar background of methane [10]. Control of trace amounts of background gas may be important in reaching the highest performances in ion traps. The best alternative is total elimination through source identification or perhaps cryogenic vacuums. An improved vacuum resulting in an increased confinement lifetime may also alleviate limitations due to number fluctuations.

C. Magnetics

The Zeeman energy levels of the ground state of $^{199}Hg^+$ as a function of magnetic field are shown in Fig. 6(a). The clock transition $^2S_{1/2}(F = 0, m = 0)$ to $^2S_{1/2}(F = 1, m = 0)$ is field-independent to the first order. The second-order field dependence is

$$\nu(B) = 40.507347997 \text{ GHz } + 97B^2 \left[\frac{\text{Hz}}{\text{G}^2}\right] \qquad (3)$$

The fractional sensitivity of this transition to magnetic field variations is more than 800 times less than that of hydrogen and nearly 20 times less than with cesium at the same operating field. A Helmholtz coil centered on the trapping region is used to apply a constant magnetic field B. The minimum operating field depends upon the field homogeneity and interrogation time. Presently the operating field must be $\geq$ 35 mG. At 35 mG, the unshielded atomic sensitivity is 1.7×10^{-13}/mG. To reach 1×10^{-16} frequency stability, the current in the Helmholtz-field bias coils must be stable to 2×10^{-5}. To prevent ambient field disturbances from influencing the ion hyperfine frequency, the trap region is surrounded by a triple-layer magnetic shield with a shielding factor specified to be $\geq$ 10,000. With this shielding factor, changes as large as 5 mG would lead to a 1×10^{-16} fractional frequency shift.

Fluctuations in the ambient magnetic field are typically less than 1 mG peak to peak. It is useful to examine these fluctuations over time and infer an equivalent Allan deviation (i.e., fractional frequency) to the magnetic environment. Figure 7(a) shows measurements of magnetic fluctuations averaged over time and scaled with the trapped ion sensitivity (for B = 50 mG and a shielding factor of 10,000). This trace exemplifies the inherent insensitivity of the mercury ion standard to magnetic field fluctuations. Currently, magnetic fluctuations are not a limiting systematic until below 10^{-16} stability.

Magnetic gradients are more of an immediate concern towards reaching higher frequency stability since gradients over the ion cloud will degrade atomic coherence and limit

line Q. The linear trap geometry is susceptible to field inhomogeneities, and field gradients are a limitation to long interrogation times. Even though the materials of the trap are carefully selected for their nonmagnetic properties, small paramagnetism of the trap, vacuum enclosure, and supporting materials result in small gradients across the ion cloud. On the same order, gradients also result from the field produced by the Helmholtz coils that are located inside the magnetic shields. To achieve high line Q, a partial solution has been to operate the standard in a relatively high magnetic field ($\geq$ 35 mG).

A related situation resulting in loss of line Q is shown in Figs. 6(b) and 6(c). In this case, the Ramsey signal is lost when the Zeeman splitting of the magnetic states $^2S_{1/2}(F = 1, m = \pm 1)$ is near the ion motional frequency of 500 kHz. This region must be avoided by proper choice of the trapping frequency in relation to the operating magnetic field.

D. Optical Pumping and Detection System

The optical pumping for state selection and interrogation with 194-nm light is a most critical area, one where improvements may lead to substantial gains in performance through increased SNR. The greatest difficulty is minimizing unwanted scattered light due to the use of a lamp as the optical pumping light source. Laser excitation would greatly improve the SNR through low background rates. Unfortunately, laser systems at 194 nm are not presently suitable for practical frequency standards that perform with long-term stability. With the present optics system, the achieved SNR is typically 40.

The lamp is dimmed during the Ramsey interrogation, since a light shift of $1.2 \times 10^{-15}/1000$ counts is observed. The typical counts during each interrogation result in an offset of 10^{-15}, though fluctuations in the count number are an order of magnitude lower.

E. Microwave Source: Local Oscillator

The multiplier chain (100 MHz–40.5 GHz), amplifiers, cabling, and waveguide to generate and transport the approximately 40.5-GHz microwave signal to drive the Hg^+ transition are not thermally regulated in the current apparatus. Because of the high degree of temperature control in the Frequency Standards Laboratory (FSL), this has not been a limitation at JPL. The microwave source did show sensitivity to temperature fluctuations during recent tests at Goldstone station DSS 13. An engineering version will need thermal regulation.

The short-term performance of the passive ion trap standard is dependent on the local oscillator (LO) and multipliers used to produce 40.5 GHz. Hydrogen masers, excellent quartz crystals [2,3], and the JPL superconducting cavity maser oscillator (SCMO) have been used as the LO. In a free-run mode, stability is limited by the LO, and for practical purposes this mode of operation is only valuable for diagnostics and systematic measurements. With feedback, all three of these sources have been steered, and in principle compensate for environmental shifts in the LO.

F. Temperature Shifts

At the present time, no thermal regulation is incorporated into the ion standard itself, and only the helium-leak heater is actively regulated. The fractional temperature sensitivity of the complete system is less than 10^{-14}/deg C as measured by varying the temperature in one of the test chambers at JPL's FSL. Using this sensitivity, the temperature control in the test chamber is displayed in Fig. 7(b) as an inferred Allan deviation. Most of the measured sensitivity seems due to an increase in neutral mercury vapor and a consequent increase in ion number (and therefore cloud radius and second-order Doppler shift). The mercury lamp and its housing must also be temperature controlled because the 194-nm UV brightness is highly dependent on the operating temperature. In the present version, the temperature and local atmosphere are controlled by blowing dry nitrogen gas over the tip of the bulb, which controls the ^{202}Hg pressure and prevents ozone formation around the lamp.

Since the lamp (on average $\leq$ 7 W) is inside the magnetic shields, the equilibrium-operating temperature depends on the duty cycle of the lamp operation. The time constant for the lamp and surrounding apparatus to reach thermal equilibrium is about 3 hr after starting with new settings. A recent addition of a nonmagnetic shutter constructed from a piezoelectric bimorph now allows the lamp to run continuously, which eliminates temperature fluctuations when changing to different duty cycles. Small temperature changes in the vacuum enclosure would also slightly raise the equilibrium helium temperature, though the second-order Doppler shift due to thermal motion is significantly lower than the shift due to the trapping fields (Fig. 8).

The neutral mercury pressure in the trap region depends on the temperature of the HgO source and on the details of the sublimation process, which may vary with time. Temperature control on the heater is currently about 0.2 deg C out of 200 deg C. Higher regulation is needed, though an active ion-number control would eliminate the need for high regulation on this heater and the reliance on the stability of the HgO sublimation process and rate.

G. Transportability and Vibration Sensitivity

In order to determine sensitivity to transportation and actual field conditions, the unit was transported to the Goldstone complex and operated at DSS 13. The "laboratory" unit successfully demonstrated transportability, and the complete system was operational less than 24 hr after arrival at Goldstone from a cold start. The overall performance was similar to that at the FSL. Since no thermal regulation was integrated into the standard, temperature fluctuations at DSS 13 were the limiting systematic.

The ion trap was under study in the FSL during the June 28, 1991 magnitude-5.8 earthquake. Table 2 shows the relative frequency shift between frequency standards under test at the FSL and to the NIST time scale via the Global Positioning System (GPS). The JPL hydrogen masers DSN2 and DSN3 showed large shifts, while the ion trap showed no shift with respect to the commercial standards by HP (Cesium clock) and SAO (Hydrogen Maser) as well as the NIST (GPS) reference. Unlike these commercial standards, the present "laboratory" version of the ion trap has no vibration isolation incorporated. The earthquake exemplifies the insensitivity of the trapped ion standard to mechanical stress and low-frequency vibration.

IV. Summary

Short-term performance can best be improved by increased SNR and higher line Q. Improved optical systems and geometries offer the most promise for achieving significant improvements in SNR. Improved magnetic homogeneity and vacuum control are the most critical areas for achieving even higher line Q's.

The environmental sensitivity of the JPL linear ion trap frequency standard has been measured. The long-term stability depends on the sensitivity of the atomic system to changes in environmental and operating parameters and on the ability to control and stabilize such parameters. The major frequency offsets under current operating conditions are summarized in Fig. 8, and the system sensitivities, present regulation, and regulation required for a stability of 10^{-16} are summarized in Table 1. The ion trap serves as a practical high-performance frequency standard with long-term stability as good as the regulation will allow. Long-term regulation of the ion number appears to be the most immediate challenge in reaching higher frequency stabilities. In the present mode of operation, further temperature regulation of the HgO heater will help, though active ion-number stabilization may be required.

A second system now under development will entail a higher degree of regulation and engineering, which is expected to improve long-term performance. Since measurements greater than 24,000 sec are already limited by the reference hydrogen masers [2,3], this second system will also provide the means for measuring and quantifying the achievable long-term stability with ion trap technology.

Acknowledgments

The authors thank W. Diener, A. Kirk and R. Taylor for assistance with the Frequency Standards Laboratory (FSL) Test and Measurement System and R. Wang and C. Greenhall for acquisition and determination of the inferred Allan deviations for magnetic and temperature fluctuations at the FSL.

References

[1] F. G. Major and G. Werth, "Magnetic Hyperfine Spectrum of Isolated $^{199}Hg^{+}$ Ions," *Appl. Phys.*, vol. 15, pp. 201–208, January 1981.

[2] J. D. Prestage, R. L. Tjoelker, G. J. Dick, and L. Maleki, "Ultra-Stable Hg^{+} Trapped Ion Frequency Standard," in special issue on trapped ions, *J. Mod. Opt.* (1992); in press.

[3] J. D. Prestage, R. L. Tjoelker, G. J. Dick, and L. Maleki, "A High-Performance Hg^{+} Trapped Ion Frequency Standard," *TDA Progress Report 42-108*, vol. October–December, Jet Propulsion Laboratory, Pasadena, California, pp. 10–18, February 15, 1992.

[4] N. F. Ramsey, *Molecular Beams*, New York: Oxford University Press, 1956.

[5] J. D. Prestage, G. J. Dick, and L. Maleki, "New Ion Trap for Frequency Standard Applications," *J. Appl. Phys.*, vol. 66, no. 3, pp. 1013–1017, August 1989.

[6] J. D. Prestage, G. J. Dick, and L. Maleki, "The JPL Trapped Mercury Ion Frequency Standard," *TDA Progress Report 42-92*, vol. October–December, Jet Propulsion Laboratory, Pasadena, California, pp. 13–19, February 15, 1988.

[7] R. K. Melbourne, J. D. Prestage, and L. Maleki, "Inhomogeneous Electric Field Effects in a Linear RF Quadrupole Trap," *TDA Progress Report 42-101*, vol. January-March, Jet Propulsion Laboratory, Pasadena, California, pp. 51–57, May 15, 1990.

[8] L. S. Cutler, R. P. Giffard, and M. D. McGuire, "Thermalization of ^{199}Hg Ion Macromotion by a Light Background Gas in an RF Quadrupole Trap," *Appl. Phys.*, vol. B 36, pp. 137–142, March 1985.

[9] J. Vetter, M. Stuke, and E. W. Weber, "Hyperfine Density Shifts of $^{137}Ba^{+}$ Ions in Noble Gas Buffers," *Z. Physik*, vol. A 273, no. 2, pp. 129–135, 1975.

[10] J. J. Bollinger, D. J. Heinzen, W. M. Itano, S. L. Gilbert, and D. J. Wineland, "A 303-MHz Frequency Standard Based on Trapped Be^{+} Ions," *IEEE Trans. Instr. Meas.*, vol. 40, no. 2, pp. 126–128, April 1991.

Table 1. Present sensitivity and regulation of the trapped Hg^+ frequency standard.

Systematic	Sensitivity	Present regulation[a]	Required for 10^{-16} stability[b]
Temperature			
FSL chamber (23 deg C)	$\left(\frac{\Delta\nu}{\Delta T}\right)\frac{1}{\nu} = -9 \times 10^{-15}\left[\frac{1}{\text{deg C}}\right]$	$\Delta T \leq 0.08$ deg C	$\Delta T \leq 0.01$ deg C
Magnetic field			
Helmholtz supply ($B = 35$ mG)	$\left(\frac{\Delta\nu}{\Delta B}\right)\frac{1}{\nu} = 1.7 \times 10^{-13}\left[\frac{1}{\text{mG}}\right]$	$\frac{\Delta I}{I} \leq 2 \times 10^{-6}$	$\frac{\Delta I}{I} \leq 2 \times 10^{-5}$
Ambient fluctuation ($\Delta B_{\text{out}} \leq 5$ mG)		$\frac{\Delta B_{\text{in}}}{\Delta B_{\text{out}}} \approx 10^{-4}$	$\frac{\Delta B_{\text{in}}}{\Delta B_{\text{out}}} \leq 10^{-4}$
Pressure			
Helium ($P = 8 \times 10^{-6}$ mbar)	$\left(\frac{\Delta\nu}{\Delta P}\right)\frac{1}{\nu} = 1.1 \times 10^{-13}\left[\frac{1}{10^{-5}\text{ mbar}}\right]$	$\frac{\Delta P}{P} \leq 0.009$	$\frac{\Delta P}{P} \leq 0.001$
Second-order Doppler (ion-number dependence)			
Endcap potential ($V \geq 10$ V)	$\left(\frac{\Delta\nu}{\Delta V}\right)\frac{1}{\nu} = -2.4 \times 10^{-15}\left[\frac{1}{\text{V}}\right]$	$\Delta V \leq 1$ mV	$\Delta V \leq 1$ mV
($V \leq 6$ V)	$\left(\frac{\Delta\nu}{\Delta V}\right)\frac{1}{\nu} = -2.5 \times 10^{-13}\left[\frac{1}{\text{V}}\right]$	$\Delta V \leq 1$ mV	$\Delta V \leq 0.3$ mV
Filament emission (300μA)	$\left(\frac{\Delta\nu}{\Delta I}\right)\frac{1}{\nu} = -1.2 \times 10^{-15}\left[\frac{1}{\mu\text{A}}\right]$	$\frac{\Delta I}{I} \leq 3 \times 10^{-3}$	$\frac{\Delta I}{I} \leq 3 \times 10^{-4}$
HgO heater (≈ 200 deg C)($V \geq 10$ V)	$\left(\frac{\Delta\nu}{\Delta T}\right)\frac{1}{\nu} = -2 \times 10^{-14}\left[\frac{1}{\text{deg C}}\right]$	$\Delta T_{\text{HgO}} \leq 0.2$ deg C	$\Delta T_{\text{HgO}} \leq 0.004$ deg C
($V \leq 6$ V)	$\left(\frac{\Delta\nu}{\Delta T}\right)\frac{1}{\nu} = -8 \times 10^{-15}\left[\frac{1}{\text{deg C}}\right]$	$\Delta T_{\text{HgO}} \leq 0.2$ deg C	$\Delta T_{\text{HgO}} \leq 0.01$ deg C
Light shift			
Dim lamp (≈ 3000 Hz)	$\left(\frac{\Delta\nu}{\Delta\gamma}\right)\frac{1}{\nu} = 1.2 \times 10^{-16}\left[\frac{1}{100\text{ Hz}}\right]$	$\frac{\Delta\gamma}{\gamma} \leq 0.07$	$\frac{\Delta\gamma}{\gamma} \leq 0.03$

[a] Peak-to-peak fluctuation or drift over 2×10^5 sec.
[b] Worst-case assumes no averaging of fluctuations.

Table 2. Permanent frequency offset of Frequency Standards Laboratory clocks as compared with hydrogen masers DSN2 and DSN3, which resulted from the 5.8-magnitude earthquake of June 28, 1991.

DSN2 versus DSN3	4×10^{-11}
DSN3 versus HP 5061B (cesium)	$-2.05(5) \times 10^{-12}$
DSN3 versus SAO26 (H-maser)	$-2.05(5) \times 10^{-12}$
DSN3 versus JPL LIT (Hg^+ linear ion trap)	$-2.06(5) \times 10^{-12}$
DSN3 versus NIST/GPS	$-1.97(5) \times 10^{-12}$

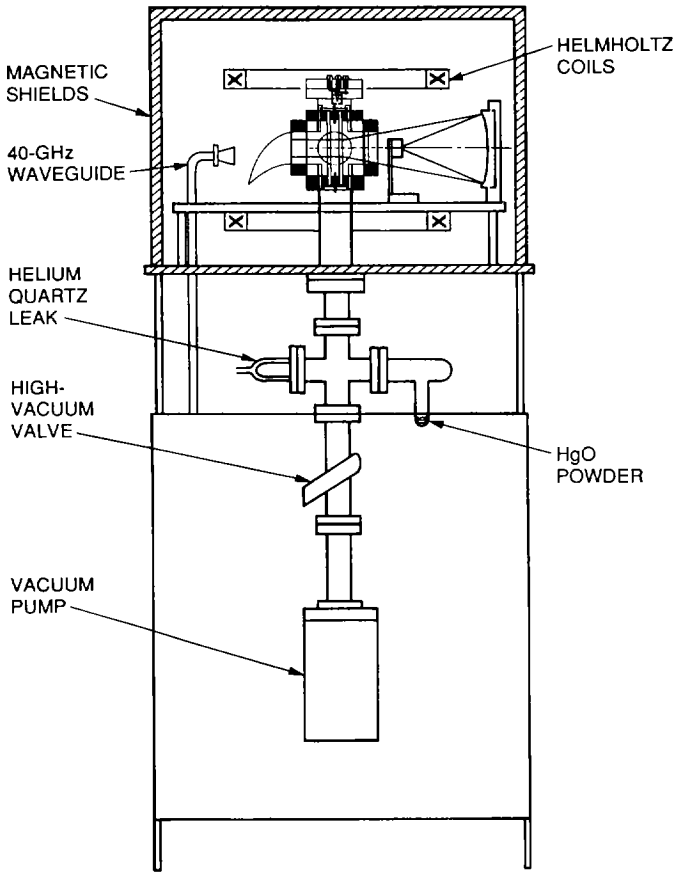

Fig. 1. Linear ion-trap frequency standard. State selection light from the ^{202}Hg discharge lamp enters from the right and is collected in a pyrex horn. Fluorescence from the trapped ions is collected in a direction normal to the page.

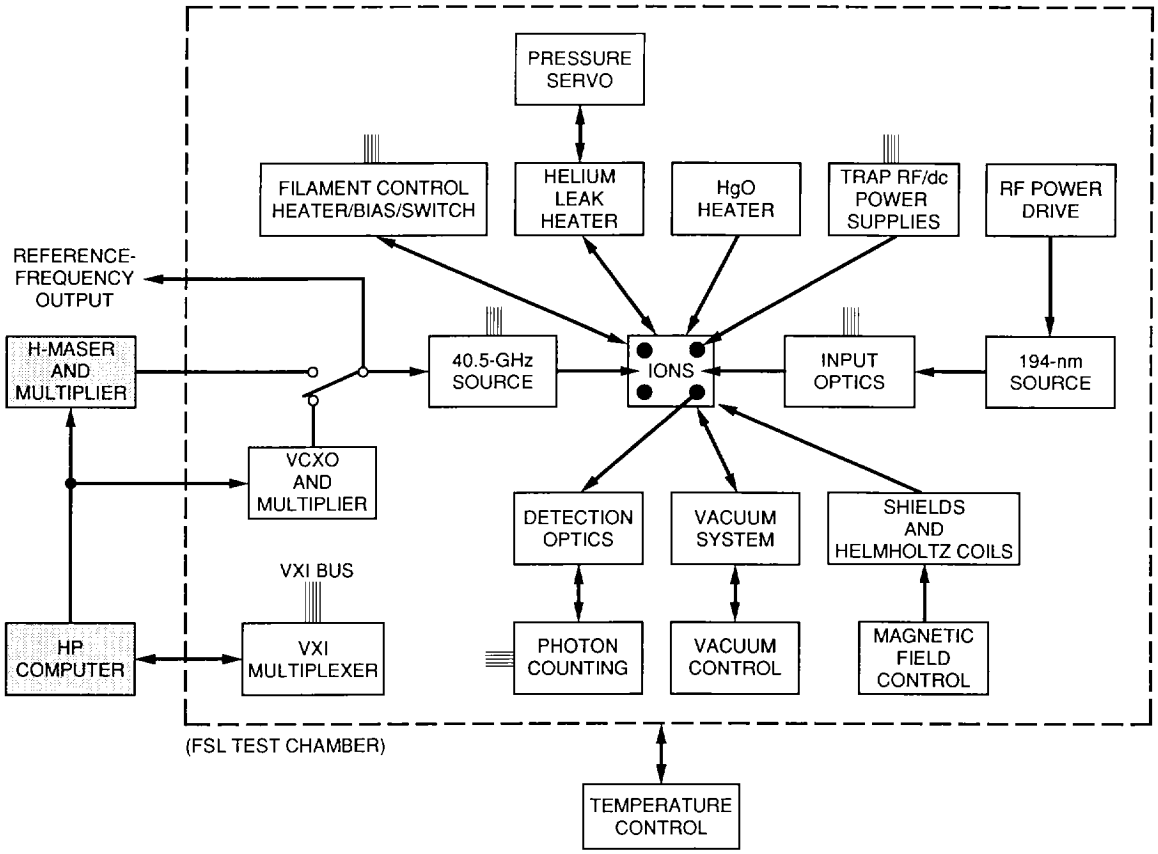

Fig. 2. The standard showing key components and subsystems.

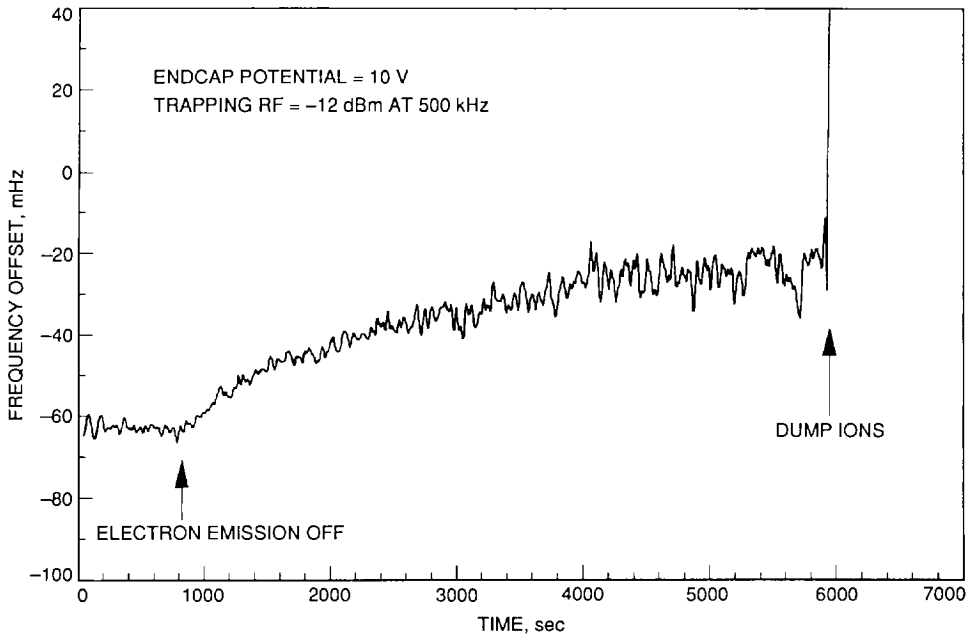

Fig. 3. A direct measure of the second-order Doppler shift due to ion motion in the rf trapping fields. As the trapped ion number diminishes, the clock frequency increases.

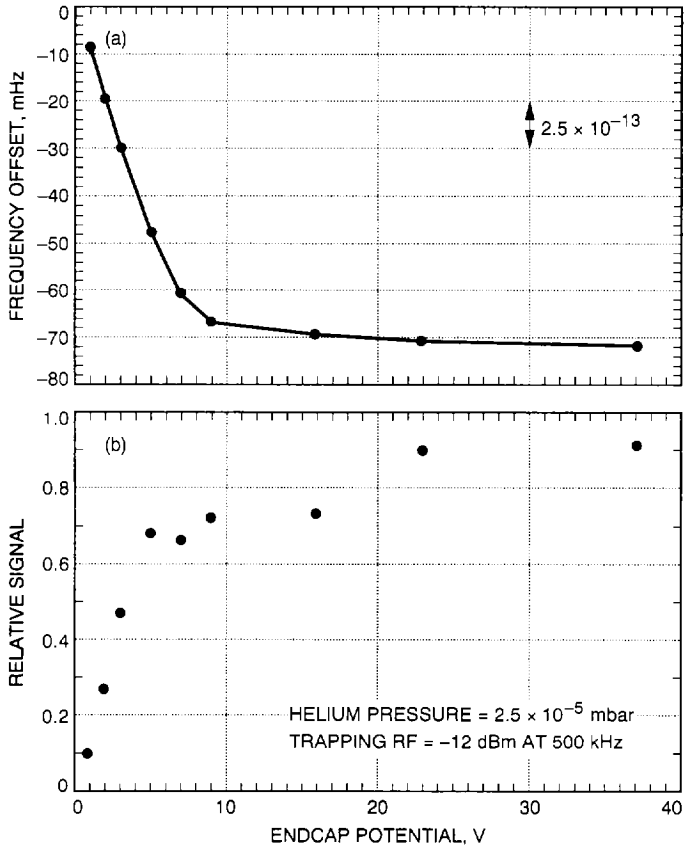

Fig. 4. Observed variations as a function of endcap potential: (a) fractional frequency offset of the clock transition and (b) signal peak amplitude.

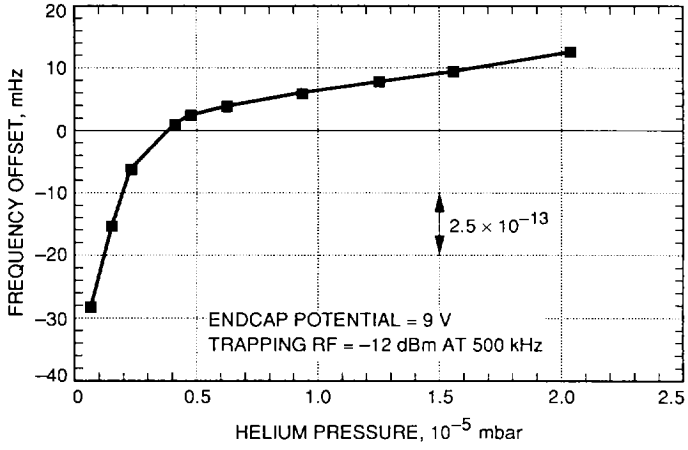

Fig. 5. The fractional frequency offset versus helium-buffer gas pressure in the trap region.

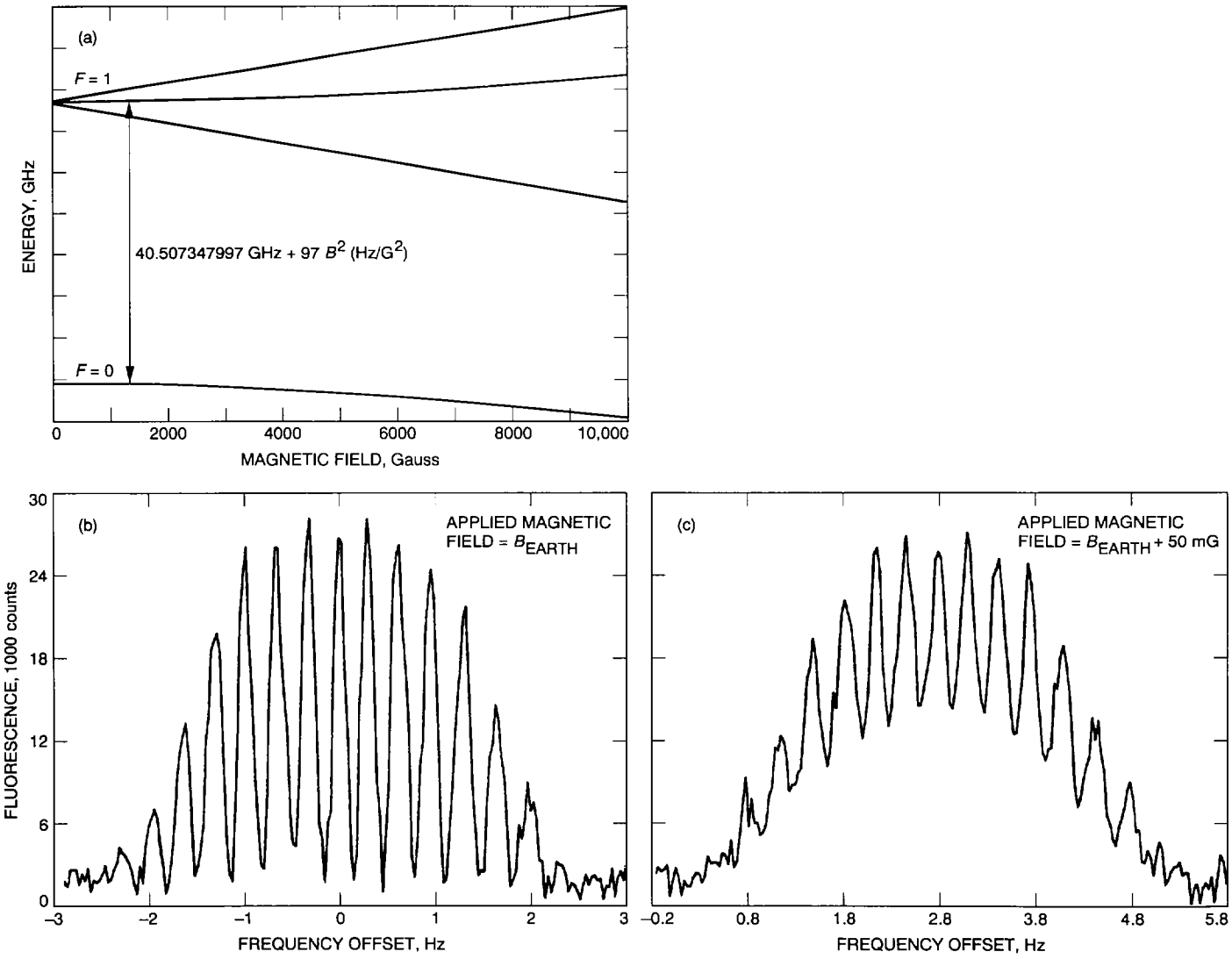

Fig. 6. Ground state transition in $^{199}Hg^{+}$: (a) schematic energy levels as a function of magnetic field; (b) typical line shape using the Ramsey method of successive oscillatory fields, with coherence preserved over the interrogation time τ = 2.5 sec; and (c) loss of coherence with the Zeeman splitting tuned nearly on resonance with the ion micromotion of 500 kHz.

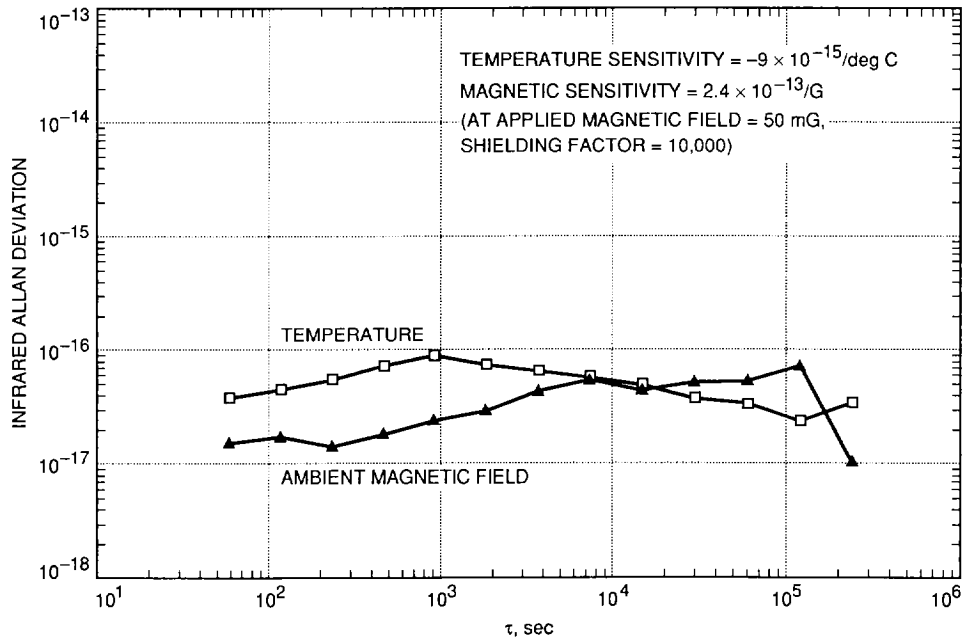

Fig. 7. Inferred Allan deviation based on: (a) magnetic and (b) temperature fluctuations measured in one of the environmental control chambers at the JPL's FSL. The plots are scaled by using the measured environmental sensitivity of the trapped ion frequency standard.

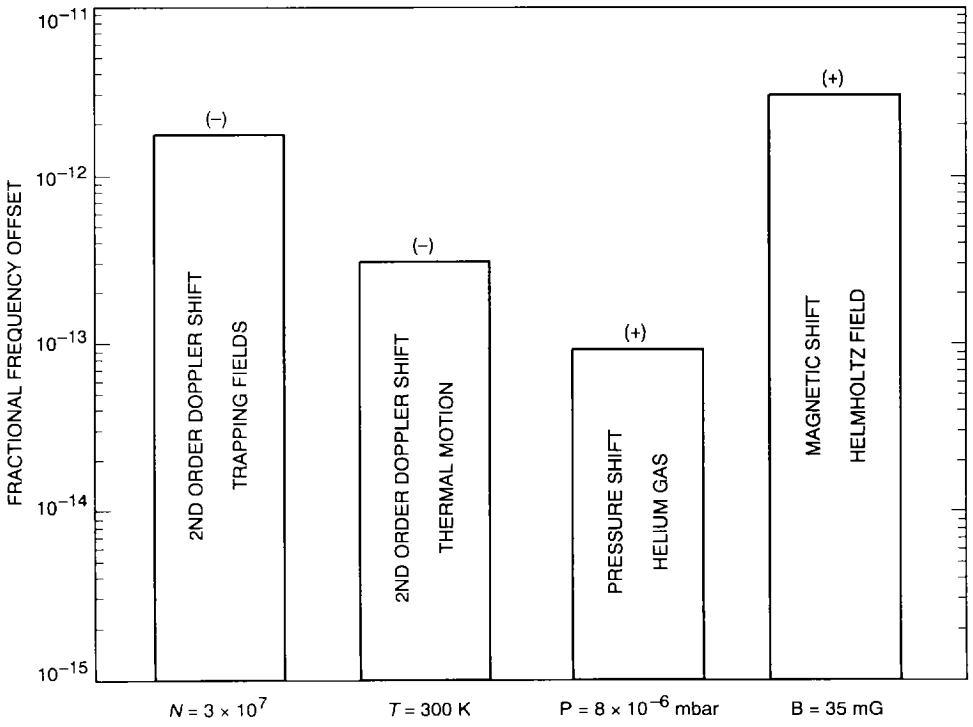

Fig. 8. The largest fractional frequency offsets to the $^{199}Hg^{+}$ clock transition in the linear trap under present operating conditions.